OAK RIDGE
NATIONAL LABORATORY
MANAGED BY UT-BATTELLE
FOR THE DEPARTMENT OF ENERGY

ORNL/TM-2014/62

ASSESSMENT OF NICKEL CLAD ALLOY 214 AS THE OUTER CONTAINMENT MATERIAL OF A FISSION CHAMBER

February 2014

D. F. Wilson

UT-BATTELLE
ORNL-27 (4-00)

ORNL/TM-2014/62

Materials Science and Technology Division

ASSESSMENT OF NICKEL CLAD ALLOY 214 AS THE OUTER CONTAINMENT MATERIAL OF A FISSION CHAMBER

D. F. Wilson

Date Published: February 2014

Prepared by
OAK RIDGE NATIONAL LABORATORY
Oak Ridge, Tennessee 37831-6285
managed by
UT-Battelle, LLC
for the
U.S. DEPARTMENT OF ENERGY
under contract DE-AC05-00OR22725

CONTENTS

Page

LIST OF FIGURES. v

LIST OF TABLES. vii

EXECUTIVE SUMMARY.. ix

1.0 INTRODUCTION. 1

2.0 EXPERIMENTAL. 5
- 2.1 TEST ARTICLE PREPARATION. 5
- 2.2 HIGH TEMPERATURE ANNEAL. 5
- 2.3 POST PROCESSING EVALUATIONS. 6

3.0 RESULTS AND DISCUSSION. 7
- 3.1 MATERIALS COMPOSITION. 7
- 3.2 NICKEL COATING. 7
- 3.3 INITIAL COATING EVALUATION. 8
- 3.4 HIGH TEMPERATURE ANNEAL. 9
- 3.5 POST ANNEAL EVALUATION. 10
  - 3.5.1 Metallography. 10
  - 3.5.2 Quantitative Analysis. 10
  - 3.5.3 Thickness Requirements. 13

4.0 CONCLUSIONS.. 15

5.0 ACKNOWLEDGMENTS.. 17

6.0 REFERENCES.. 19

APPENDIX A. A-1

LIST OF FIGURES

Figure **Page**

Fig. 1. Cross-sections of nickel clad Alloy 214. The specimens were clad using the MOCVD process, which was not optimized to obtain a uniform coating. . 8

Fig. 2. Specimens encapsulated in quartz a) before 850°C, 1000 h anneal; and b) after 850°C, 1000 h anneal.. 9

Fig. 3. Typical appearance of cross-sections of nickel clad Alloy 214 after a 850°C, 1000h anneal in argon-4% hydrogen: a) low mag. and b) higher mag. Some porosity has developed as a result of reordering of the morphology of the nickel layer.. 10

Fig. 4. Image showing location of the elemental line scan and position of the interface between Alloy 214 and the nickel cladding with respect to the start of the line scan.. 11

Fig. 5. Normalized elemental concentration (at %) as a function of distance. The interface between Alloy 214 and the nickel cladding is at 188 μm.. 12

Fig. A.1. Image showing location of the elemental line scan across a gap in the interface and position of the interface between Alloy 214 and the nickel cladding with respect to the start of the line scan A-6

Fig. A.2. Normalized elemental concentration (at %) as a function of distance across gap interface. The interface between Alloy 214 and the nickel cladding is at 250 μm.. . . . . A-7

LIST OF TABLES

TABLE **Page**

Table 1. Nominal composition (wt.%) of alloys of interest. 2

Table 2. Nominal composition (wt.%) of Alloy 214 and measured composition of the substrate. 7

Table A.1. Elemental concentration (at. %) across smooth interface of Alloy 214 and nickel cladding. A-1

Table A2. Elemental concentration (at. %) across gap interface of Alloy 214 and nickel cladding. A-7

EXECUTIVE SUMMARY

Fission chambers are being designed to monitor in-core reactor power level via measurements of neutron flux from startup through full power. These fission chambers are being design to operate at coolant temperatures that range from 700°C (FLiBe-cooled) to 800°C (helium-cooled reactors) with some additional heating due to the presence of high fluxes of neutrons. The additional heat can increase the internal temperature of the fission chamber by approximately 200 degrees Celsius. These high temperatures and dissimilar coolants present significant and different challenges for the design of the fission chambers. Yet, it is highly desirable to have one design and manufacturing process for a fission chamber. In such a design, high-temperature creep strength and chemical compatibility with both helium with controlled levels of impurities and liquid fluoride salt environments are needed. Nickel (chemical compatibility with helium with controlled levels of impurities, and liquid fluoride salt) coated Alloy 214 (high-temperature creep strength) was evaluated for use as the external containment material of the fission chamber.

Alloy 214 was coated using vapor deposition from nickel carbonyl. The coated specimens were subjected to a high-temperature anneal at 850°C for 1000 h. Post-processing evaluations included dimensional and gravimetric analyses, metallography, and electron probe micro-analysis.

The results this evaluation demonstrated:

- Vapor deposition of nickel based on the nickel carbonyl process successfully coated all surfaces of a high-temperature, nickel-based parallelepiped specimen.
- The high-temperature anneal of the coated specimen in the absence of FLiNaK

successfully allowed for the determination of lifetimes and calculation of thickness needed for the proposed two year lifetime of the fission chamber.

- For the average thickness achieved by an un-optimized coating process, a lifetime of 0.55 to 0.63 y at 850°C can be achieved.
- For a lifetime of 2 years at 850°C, a nickel coating of thickness 3600 to 4111 μm (3.6 to 4.1 mm) is required; and for a lifetime of 1 year at 850°C, a thickness of 1800 to 2100 μm (1.8 to 2.1 mm) is required.
- The required nickel-coating thickness for the external surfaces of the fission chamber for the desired lifetimes can be achieved with reasonable residence times using internal heating of the chamber and optimized process parameters for the nickel carbonyl vapor deposition process.

1.0 INTRODUCTION

In-core fission chambers are being designed to monitor reactor power level via measurements of neutron flux from startup through full power in flowing molten FLiBe-cooled or flowing helium-cooled high-temperature reactors. The chamber will experience external temperatures as high as 700°C and 800°C in FLiBe-cooled and helium-cooled reactors, respectively. In addition, the internals of the chamber, which will be exposed to a noble gas-nitrogen mixture, will experience an approximate 200 degrees Celsius higher temperature due to the presence of high fluxes of neutrons.

These high temperatures present significant challenges for the mechanical design of the chambers, and the dissimilar coolant environments impose different requirements on materials compatibility. The high pressure associated with the helium-cooled environment imposes significantly higher requirements on the high-temperature creep behavior of the materials of construction as compared with the FLiBe-cooled environment. While both coolants require careful control of coolant chemistry for long-term materials compatibility, materials compatibility in the helium-cooled environment is dependent on the formation of a very slow-growing protective oxide layer on alloys, and that in FLiBe-cooled environment is highly dependent on materials being thermodynamically stable with respect to the coolant. In general, alloys that demonstrated good materials performance at high temperatures were designed for use in oxidizing environments. These alloys contain chromium and/or aluminum that provide for the high-temperature oxidation resistance. In a fluoride salt environment at high temperature, chromium and aluminum readily partition into the salt, especially if there is inadequate control of the redox potential of the salt. While there is an alloy, INOR-8, developed at ORNL for use with FLiBe and now marketed as Hastelloy® N, its use is limited to temperatures less than 704°C

due to inadequate creep strength at higher temperatures. The compositions of Haynes® 214® (Alloy 214) a high-temperature, high-strength alloy, and Hastelloy® N (Alloy N) and are presented in Table 1. As shown, there are significantly more chromium and aluminum in Alloy 214 as compared to Alloy N. The different environments associated with the two reactors strongly suggest the use of different high-temperature alloys as materials of construction of the fission chamber. However, the ability to use one design and manufacturing process for a fission chamber that can be used in either environment is highly desirable.

Table 1. Nominal composition (wt%) of alloys of interest

Alloy	Ni	Fe	Cr	Mn	Si	Al	C	B	Zr	Y	Co	Cu	W
214*	75	3	16	0.5	0.2	4.5	0.05	0.01	0.1	0.01			
N†	71	5	7	0.80	1	Al + Ti = 0.35	0.08				0.20	0.35	0.50

* http://www.haynesintl.com/pdf/h3139.pdf
† http://www.haynesintl.com/pdf/h2052.pdf

Two reports[1, 2], present the details of the design and materials of construction of the proposed fission chamber. These reports present the rationale for the materials and techniques for developing the fission chamber. The present work is an initial evaluation of a clad high-temperature, high creep-strength alloy. The substrate is Alloy 214, which provides for the high-temperature creep strength, that is clad with pure nickel, which provides for fluoride salt corrosion resistance.

As reported previous, the Nickel Vapor Deposition process using nickel carbonyl gas as a precursor, which has been known for more than 100 years, provides for a pure nickel surface

layer.[3] In this process, nickel carbonyl gas is introduced into a deposition chamber at 50°C and is decomposed into pure nickel and carbon monoxide at temperatures close to 175°C, as shown in the equation (1):

$$Ni(CO)_4 = Ni + 4CO \quad (1)$$

2.0 EXPERIMENTAL

2.1 TEST ARTICLE PREPARATION

Specimens of Alloy 214 of approximate dimensions 0.15 by 1.01 by 1.90 cm, in thickness, width and length respectively, with a hole drilled at one end, were machined, stamped with identification marks, dimensioned, weighed, cleaned and shipped to CVRM Corporation, Toronto, Ontario, Canada, for nickel coating via a vapor deposition process. Also, one specimen was shipped to Dirats Laboratories, Westfield, MA for bulk chemical analysis.

At CVRM Corporation, the specimens were degreased using Aquanox, rinsed in de-ionized water and dried at room temperature. A red silicone sheet was cut to mask the heating plate and to prevent nickel deposition on the plate. Eight specimens were place on the heating plate inside cut-outs in the red silicone sheet. The chamber was pressure tested and then sparged first with argon, and then carbon monoxide. The heating plate was raised to a temperature of 175°C with temperature control facilitated with thermocouples placed next to the specimens. Gaseous nickel carbonyl was introduced from the top of the deposition chamber and deposition was continued for approximately 40 minutes. After the initial deposition was completed, nickel carbonyl and carbon monoxide was sparged from the chamber, and the specimens were cooled and flipped to the other side. The chamber was closed, sparged, and the coating procedure was repeated. After sparging and cooling to room temperature, the coated specimens were removed from the chamber, placed in plastic bags, and shipped to ORNL.

2.2 HIGH TEMPERATURE ANNEAL

Nickel coated specimens were sealed in quartz under approximately 0.10 atm of argon-4% hydrogen mixture. The argon-4% hydrogen mixture was employed to prevent oxidation of the

specimens during the high temperature anneal. The quartz ampoule was placed in an air furnace, heated to 850°C, and maintained at temperature for 1000 h. One thousand hours was considered to be sufficient time to allow for establishing detectable travel-distances of the diffusing elements. At the end of 1000 h, the power to the furnace was turned off, the quartz ampoule was pulled from the furnace and allowed to air cool.

2.3 POST PROCESSING EVALUATIONS

Post-processing (coating and high-temperature anneal) evaluations included dimensional and gravimetric analyses, metallographic preparation of specimens, optical microscopy, and elemental chemical analyses using an Electron Probe Micro-analyzer (EPMA), JEOL JX-8200, operated at 15kV and at probe current of 50nA.

3.0 RESULTS AND DISCUSSION

3.1 MATERIALS COMPOSITION

The evaluated composition of the substrate material is presented in Table 2. As shown, the substrate used in this evaluation has a composition that is characteristic of Alloy 214. The larger differences between nominal and measured compositions occur for elements given as maximum amount allowed in the alloy. The small amount of cobalt (most likely from the nickel source) will need to be considered in evaluating post in-reactor exposure operations.

Table 2. Nominal composition (wt%) of Alloy 214 and measured composition of the substrate

Alloy	Ni	Fe	Cr	Mn	Si	Al	C	B	Zr	Y	Co	V	O+N
Nominal*	75	3	16	0.5†	0.2†	4.5	0.05	0.01†	0.1†	0.01			
Measured‡	Bal	3.47	15.99	0.17	0.05	4.51	0.037		0.03		0.01	0.01	0.0029

* http://www.haynesintl.com/pdf/h3139.pdf
† Maximum
‡ Dirats Test Report # R569203, dated Jul 08, 2013

3.2 NICKEL COATING

CVRM Corporation employed specimens with a small hole at one end, matching the dimension of those received from ORNL, to establish the initial parameters for complete encapsulation of the specimens using the Nickel Vapor Deposition process. Complete encapsulation was a criterion for high temperature testing in the presence of FLiNaK. The first series of tests was conducted in a vertical chamber with the suspended specimens heated by radiant heat from the walls of the reactor, which was held at 210°C. Nickel carbonyl gas was introduced from the top of the deposition chamber. After several hours of deposition, the chamber was opened and coated specimens were examined. The thickness of deposited nickel was calculated from the

weight gain of the specimen and its surface area. It was determined that most of the deposition occurred on the walls of the reactor and not on the specimens. Hence, a revised procedure (described early) was developed that involved coating one side of the specimens while it was being heated on a hot plate at 175°C, flipping the specimen over, and repeating the coating process.

3.3 INITIAL COATING EVALUATION

Cross-sections of a nickel clad Alloy 214 specimen are presented in Fig. 1. As shown, the coating process, while not optimized for a uniform coating thickness, readily follows the contours of the specimens. Gaps between the nickel coatings and the substrates were observed. In some regions, these gaps were much wider than would be expected from that due to the differences in coefficient of expansion between nickel and the substrate alloy, and the thickness of native oxide on the specimen surface. Prior to the deposition process, no attempt was made to remove the native oxide on the surface of the specimens. As there was excellent interfacial contact in most regions and the substrate was completely encapsulated in nickel, the decision was made to proceed with a high-temperature anneal.

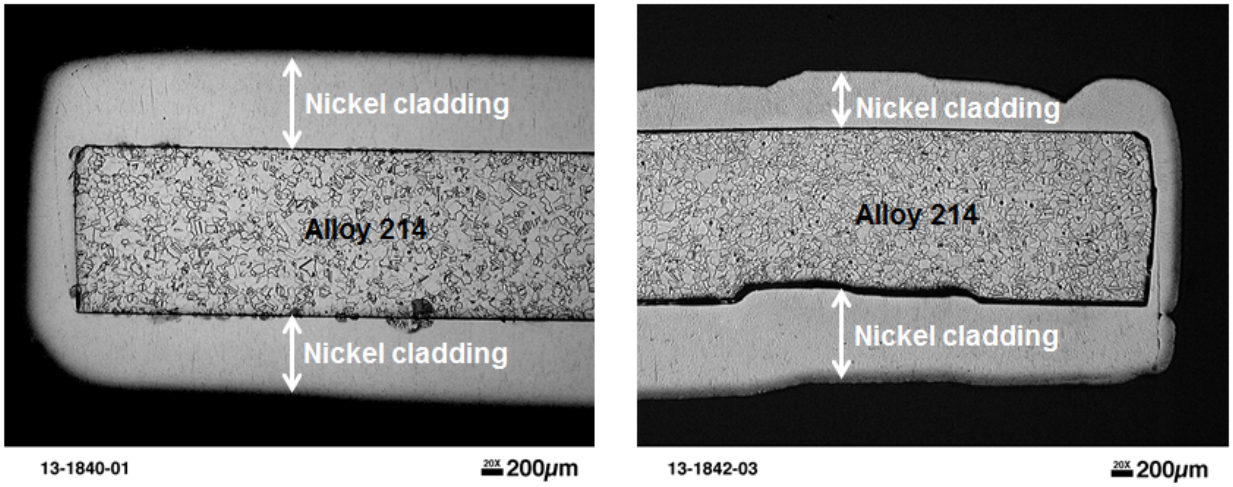

Fig. 1. Cross-sections of nickel clad Alloy 214. The specimens were clad using the MOCVD process, which was not optimized to obtain a uniform coating.

3.4 HIGH TEMPERATURE ANNEAL

The initial intent was to expose the specimens to FLiNaK salt at high temperature in individual molybdenum capsules. Unforeseen and unfortunate events voided the subcontractor ability to provide capsules loaded with clean FLiNaK in a timely manner. This forced the abandonment FLiNaK testing in the interest of meeting the programmatically mandated schedule. Therefore, the decision was made to anneal the nickel-clad Alloy 214 specimens in quartz in an Ar-H_2 atmosphere, which would prevent oxidation of the specimen. Although this approach does not allow for a constant chemical activity at the nickel/salt interface as a result of partitioning of diffusing elements into the salt, it permits a determination of diffusion distances. The specimens, sealed in quartz, are shown in Fig. 2. After the anneal, the outside of the quartz ampoule, shown in Fig. 2 b), had undergone some devitrification (a whitish byproduct) in the air environment of the furnace. There were no apparent effects inside the ampoule.

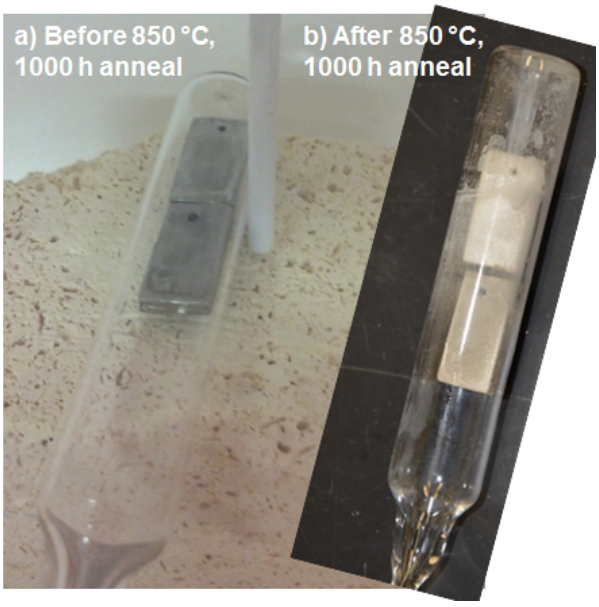

Fig. 2. Specimens encapsulated in quartz a) before 850°C, 1000 h anneal; and b) after 850°C, 1000 h anneal.

3.5 POST ANNEAL EVALUATION

3.5.1 Metallography

Cross-sections of the nickel coated Haynes 214 specimen are presented in Fig. 3. As shown, the outer nickel layer has developed some porosity as a result of reordering of its morphology. This significant change in morphology (compare Fig. 1 to Fig. 3) is expected, as this anneal was the first exposure of the nickel coat to high temperature (850°C). The average thickness of the coating before the anneal was 1036 μm and the average thickness of the coating after the anneal was 1211 μm. An average of these two averages was used for calculation of coating lifetimes.

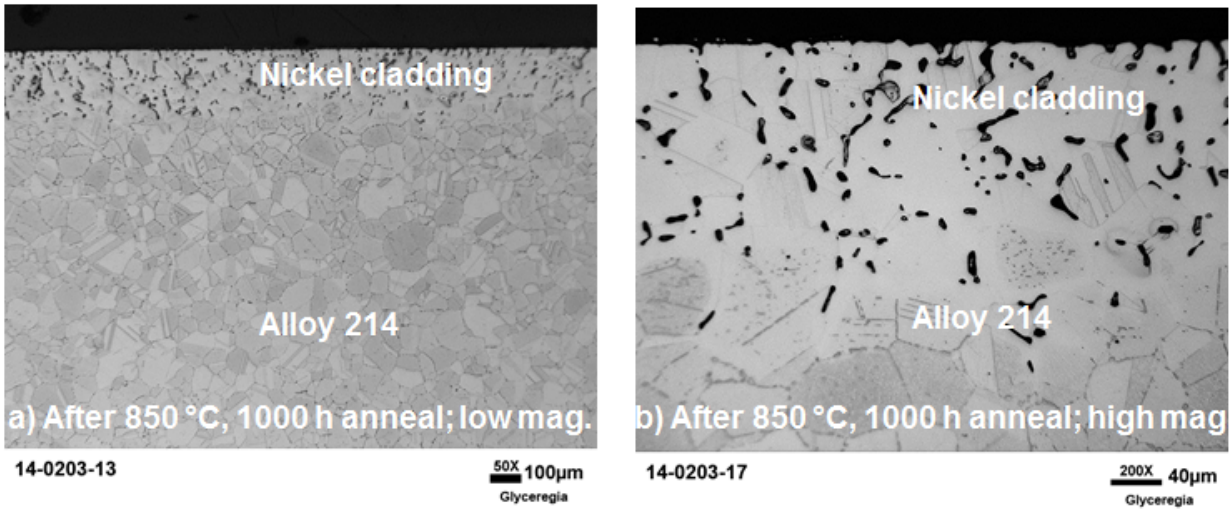

Fig. 3. Typical appearance of cross-sections of nickel clad Alloy 214 after a 850°C, 1000h anneal in argon-4% hydrogen: a) low mag. and b) higher mag. Some porosity has developed as a result of reordering of the morphology of the nickel layer.

3.5.2 Quantitative Analysis

The location of the elemental line scan (red arrow) and the distance to the interface between Alloy 214 and the nickel cladding from the starting point of the line scan (blue arrow) are shown

in Fig. 4. The associated chemical information, obtained via wavelength-dispersive spectroscopy using an EPMA, is presented in Fig. 5 (The normalized atom percentage data are presented in Appendix A). As shown, the elemental concentration of the diffusing species, Cr, Al, and Fe, decreased within the base alloy within a short distance of the interface and no diffusing species arrived at the nickel/argon-4%hydrogen interface. Hence, the results are applicable to fluoride salt-cooled and the helium gas-cooled nuclear reactors. Chemical data were also obtained for a line scan that included a gap between the substrate and the nickel coating. These normalized atom percentage data and associated graph and image of the microstructure at the scan line are presented in Appendix A. The gap in the interface between the substrate and coating resulted in a much more rapid decrease in diffusing chemical species with distance.

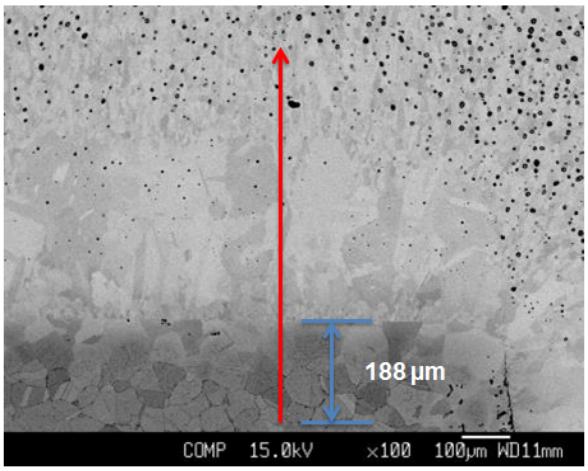

Fig. 4. Image showing location of the elemental line scan (red arrow) and position of the interface between Alloy 214 and the nickel cladding with respect to the start of the line scan (blue arrow).

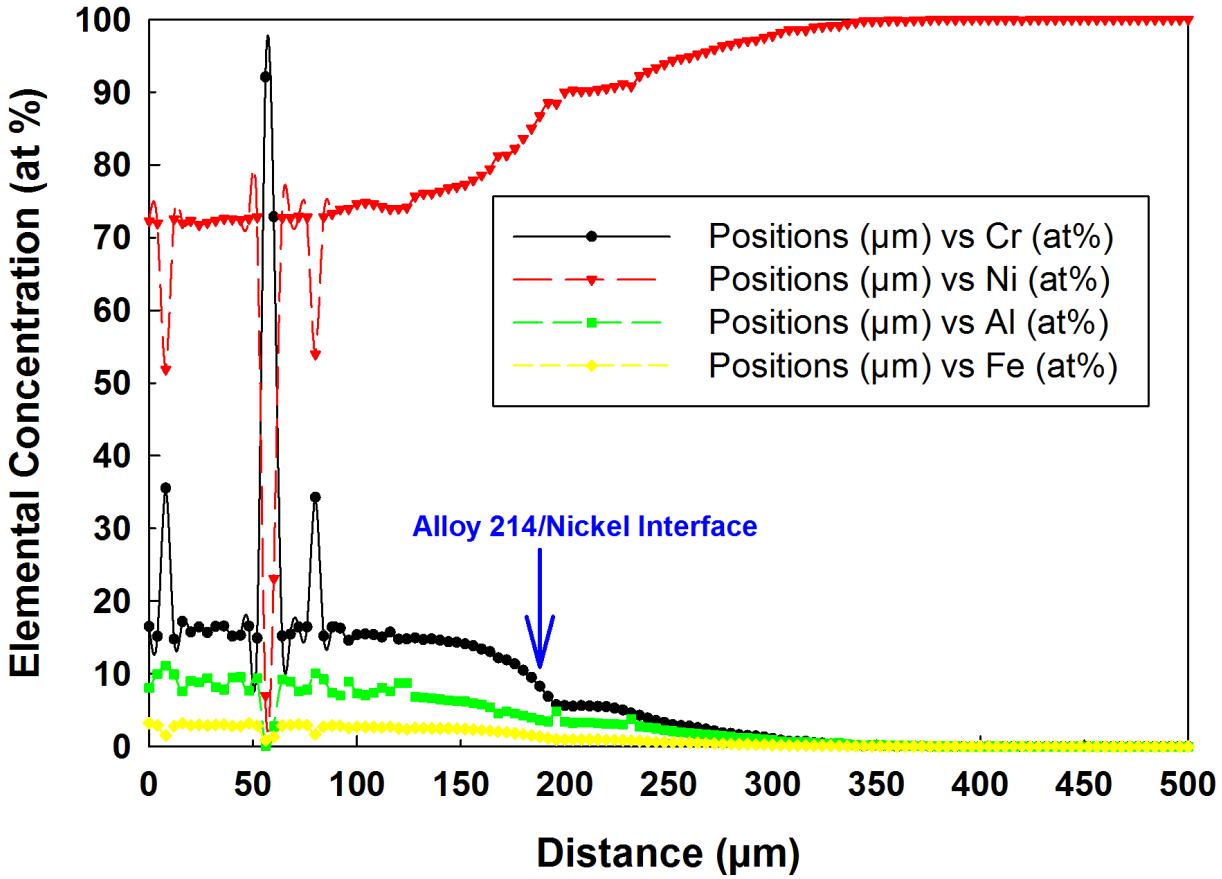

Fig. 5. Normalized elemental concentration (at %) as a function of distance. The interface between Alloy 214 and the nickel cladding (blue arrow) is at 188 μm.

As presented in Fig. 5, post-interface location, the elemental concentrations decreased in the nickel cladding to zero within 204 to 236 microns as measured with respect to the original Alloy214/nickel interface (blue arrow in Fig. 5). Using data from prior work[4] for chromium tracer (Cr^{51}) diffusion into Inconel (not stated but most likely Inconel 600) and INOR-8 (Alloy N), nickel chromium alloys, in the temperature range of 600 to 900°C, a distance of 18 microns (11 to 13 times smaller) can be calculated. Also, the authors showed a decrease in the diffusion rate of chromium with increasing chromium additions to nickel-based alloys. The larger transport

distance in the present work is due to several factors including reorientation of the morphology of the pure nickel cladding and development of porosity (contributes to the increase in thickness reported earlier) due to the high temperature anneal, and differences in cross-interactions between the diffusing species into pure nickel as compared to chromium diffusing into nickel-chromium alloys. At 850°C (less than ⅔ the melting point of nickel), increased surface area for rapid surface diffusion, as compared to volume diffusion, would significant increase the diffusion rates.

3.5.3 Thickness Requirements

The un-optimized nickel carbonyl coating process resulted in an average coating thickness (coating before anneal and coating after anneal) of 1124 μm (1.124 mm). Using this average thickness and a distance range of 204 to 236 microns for diffusing elements concentration to fall to zero, results in a lifetime [time for diffusing elements to arrive at the external nickel surface (nickel/gas interface)] of 0.55 to 0.63 y. Alternatively, a lifetime of 2 years at 850°C requires nickel coating of thickness 3600 to 4111 μm (3.6 to 4.1 mm); and that of 1 year at 850°C, a thickness of 1800 to 2100 μm (1.8 to 2.1 mm). Using internal heating of the chamber and optimized process parameter for the nickel carbonyl vapor deposition process, these coating thicknesses can be achieved with reasonable residence times.

4.0 CONCLUSIONS

The use of a nickel coated high-temperature material (Alloy 214) as the enclosure of the fission chamber was evaluated. The results this evaluation demonstrated:

- Vapor deposition of nickel based on the nickel carbonyl process successfully coated all surfaces of a high-temperature, nickel-based parallelepiped specimen. Hence, the process is well suited to coating the outer nickel-based alloy enclosure of the fission chamber.
- The high-temperature anneal of the coated specimen in the absence of FLiNaK successfully allowed for the determination of lifetimes and calculation of thickness needed for the proposed two year lifetime of the fission chamber. A lifetime of 2 years at 850°C requires nickel coating of thickness 3600 to 4111 μm (3.6 to 4.1 mm).
- During the high-temperature anneal, no diffusing species reached the nickel/argon-4% hydrogen interface. Hence, the distribution of diffusing species is characteristic of a non-equilibrium distribution that could be established if Cr, Al, and Fe were being leached from the nickel by molten salt at least as fast as they arrived at the nickel/molten salt interface.

5.0 ACKNOWLEDGMENTS

The contributions of Tyson Jordan (metallography), Donovan Leonard (EPMA), Tracie Lowe (SEM), and Adam Willoughby (procurement of materials and services, and materials preparation) are gratefully acknowledged.

6.0 REFERENCES

1. Z. W. Bell, M. J. Harrison, D. E. Holcomb, C. L. Britton, N. D. Bull, R. J. Warmack, M. J. Lance, K. J. Leonard, T. Katoh, R. G. Miller, R. T. Mayes, D. R. Giuliano, and A. M. Aaron, *Materials Selection for a High-Temperature Fission Chamber,* ORNL/LTR-2012/331, August 2012, Oak Ridge National Laboratory, Oak Ridge, Tennessee.

2. Z. W. Bell, R. J. Warmack, N. S. Kulkarni, R. G. Miller, D. F. Wilson, R. T. Mayes, D. R. Giuliano, A. M. Aaron, and D. M. Manofsky, *Preliminary Design for a High Temperature Fission Chamber,* ORNL/TM-2013/435, September 2013, Oak Ridge National Laboratory, Oak Ridge, Tennessee.

3. G. Muralidharan, D. F. Wilson, L. R. Walker, M. L. Santella, and D. E. Holcomb, *Cladding Alloys for Fluoride Salt Compatibility*, ORNL/TM-2011/95, May 25, 2011, Oak Ridge National Laboratory, Oak Ridge, Tennessee.

4. R. B. Evans, J. H. DeVan, and G. M. Watson, *Self-Diffusion of Chromium in Nickel-Based Alloys*, ORNL-2982, January 20, 1961, Oak Ridge National Report, Oka Ridge, Tennessee.

APPENDIX A

The elemental concentrations across the smooth interface are presented in Table A.1.

Table A.1. Elemental concentration (at. %) across smooth interface of Alloy 214 and nickel cladding

Position	Element				
(μm)	Cr	Ni	Al	Fe	Total
0	16.489	72.258	8.041	3.212	100
4	15.161	71.966	9.986	2.887	100
8	35.524	51.868	11.093	1.516	100
12	14.749	72.540	9.929	2.782	100
16	17.197	71.989	7.628	3.186	100
20	15.733	72.342	9.024	2.902	100
24	16.450	71.739	8.837	2.973	100
28	15.658	72.050	9.427	2.865	100
32	16.501	72.329	8.179	2.991	100
36	16.565	72.579	7.828	3.028	100
40	15.167	72.534	9.496	2.803	100
44	15.291	72.413	9.524	2.772	100
48	16.569	72.575	7.666	3.191	100
52	14.914	72.823	9.419	2.843	100
56	92.058	7.025	0.078	0.839	100
60	72.850	23.086	2.744	1.320	100
64	15.183	72.736	9.200	2.881	100
68	15.450	72.698	8.933	2.919	100
72	16.416	72.901	7.627	3.057	100
76	16.456	72.783	7.829	2.933	100
80	34.270	53.968	10.078	1.684	100
84	15.189	72.833	9.256	2.721	100
88	16.410	73.285	7.421	2.884	100
92	16.258	73.907	6.982	2.853	100
96	14.592	73.964	8.900	2.544	100
100	15.354	74.628	7.313	2.704	100
104	15.459	74.792	7.085	2.665	100
108	15.372	74.590	7.374	2.664	100
112	15.057	74.248	8.078	2.618	100
116	15.719	73.939	7.617	2.725	100
120	14.746	73.980	8.766	2.509	100
124	14.782	74.118	8.741	2.360	100
128	14.932	75.668	6.851	2.549	100
132	14.692	76.031	6.760	2.518	100
136	14.791	76.080	6.619	2.510	100
140	14.613	76.388	6.494	2.505	100
144	14.377	76.776	6.359	2.487	100

Position	Element				
(μm)	Cr	Ni	Al	Fe	Total
148	14.320	76.985	6.257	2.438	100
152	14.100	77.300	6.212	2.389	100
156	13.842	77.891	5.944	2.324	100
160	13.390	78.587	5.772	2.252	100
164	13.031	79.430	5.376	2.162	100
168	12.198	81.256	4.515	2.031	100
172	11.908	81.317	4.830	1.946	100
176	11.367	82.224	4.565	1.844	100
180	10.475	83.608	4.238	1.679	100
184	9.489	85.009	3.973	1.529	100
188	8.266	86.721	3.652	1.361	100
192	6.871	88.529	3.445	1.156	100
196	5.738	88.409	4.857	0.996	100
200	5.609	89.995	3.408	0.988	100
204	5.522	90.239	3.250	0.989	100
208	5.613	90.118	3.273	0.995	100
212	5.556	90.180	3.295	0.969	100
216	5.498	90.350	3.185	0.968	100
220	5.483	90.507	3.086	0.924	100
224	5.263	90.717	3.095	0.925	100
228	5.004	91.118	2.994	0.883	100
232	4.585	90.821	3.779	0.815	100
236	4.265	92.208	2.755	0.772	100
240	3.890	92.800	2.604	0.705	100
244	3.555	93.340	2.466	0.640	100
248	3.301	93.831	2.272	0.596	100
252	2.988	94.359	2.098	0.555	100
256	2.861	94.625	1.991	0.524	100
260	2.795	94.800	1.885	0.520	100
264	2.593	95.212	1.724	0.470	100
268	2.376	95.500	1.672	0.452	100
272	2.135	95.912	1.545	0.407	100
276	1.858	96.330	1.451	0.361	100
280	1.785	96.553	1.323	0.339	100
284	1.626	96.834	1.229	0.312	100
288	1.501	97.053	1.154	0.292	100
292	1.457	97.150	1.137	0.256	100
296	1.287	97.496	0.960	0.258	100
300	1.098	97.756	0.923	0.223	100
304	0.871	98.202	0.735	0.193	100
308	0.694	98.547	0.619	0.140	100
312	0.671	98.589	0.616	0.124	100
316	0.691	98.531	0.639	0.140	100
320	0.510	98.887	0.500	0.104	100
324	0.466	98.989	0.432	0.114	100
328	0.367	99.128	0.407	0.098	100
332	0.222	99.127	0.568	0.083	100
336	0.253	99.409	0.289	0.049	100

Position	Element				
(μm)	Cr	Ni	Al	Fe	Total
340	0.167	99.583	0.214	0.036	100
344	0.030	99.775	0.144	0.051	100
348	0.036	99.754	0.185	0.025	100
352	0.034	99.766	0.180	0.021	100
356	0.036	99.849	0.098	0.017	100
360	0.000	99.841	0.136	0.023	100
364	0.055	99.826	0.095	0.024	100
368	0.042	99.907	0.040	0.012	100
372	0.032	99.879	0.079	0.010	100
376	0.000	99.948	0.040	0.012	100
380	0.000	99.992	0.008	0.000	100
384	0.000	99.994	0.006	0.000	100
388	0.000	99.949	0.033	0.018	100
392	0.000	100.000	0.000	0.000	100
396	0.000	99.995	0.000	0.005	100
400	0.000	99.998	0.000	0.003	100
404	0.017	99.974	0.004	0.005	100
408	0.000	99.987	0.013	0.000	100
412	0.000	100.000	0.000	0.000	100
416	0.000	99.999	0.000	0.001	100
420	0.000	99.924	0.076	0.000	100
424	0.000	100.000	0.000	0.000	100
428	0.000	99.999	0.000	0.001	100
432	0.000	99.991	0.000	0.009	100
436	0.000	99.989	0.000	0.011	100
440	0.000	100.000	0.000	0.000	100
444	0.000	100.000	0.000	0.000	100
448	0.000	99.990	0.010	0.000	100
452	0.000	100.000	0.000	0.000	100
456	0.000	99.993	0.008	0.000	100
460	0.000	100.000	0.000	0.000	100
464	0.000	100.000	0.000	0.000	100
468	0.000	100.000	0.000	0.000	100
472	0.000	100.000	0.000	0.000	100
476	0.000	99.990	0.000	0.010	100
480	0.000	100.000	0.000	0.000	100
484	0.000	100.000	0.000	0.000	100
488	0.000	100.000	0.000	0.000	100
492	0.000	99.997	0.000	0.003	100
496	0.000	100.000	0.000	0.000	100
500	0.000	100.000	0.000	0.000	100
504	0.000	100.000	0.000	0.000	100
508	0.000	100.000	0.000	0.000	100
512	0.000	100.000	0.000	0.000	100
516	0.000	100.000	0.000	0.000	100
520	0.000	100.000	0.000	0.000	100
524	0.000	100.000	0.000	0.000	100
528	0.000	100.000	0.000	0.000	100

Position	Element				
(μm)	Cr	Ni	Al	Fe	Total
532	0.000	100.000	0.000	0.000	100
536	0.000	100.000	0.000	0.000	100
540	0.000	100.000	0.000	0.000	100
544	0.000	100.000	0.000	0.000	100
548	0.000	100.000	0.000	0.000	100
552	0.000	100.000	0.000	0.000	100
556	0.000	99.991	0.000	0.009	100
560	0.000	99.998	0.000	0.002	100
564	0.000	100.000	0.000	0.000	100
568	0.000	100.000	0.000	0.000	100
572	0.000	100.000	0.000	0.000	100
576	0.000	100.000	0.000	0.000	100
580	0.000	100.000	0.000	0.000	100
584	0.000	100.000	0.000	0.000	100
588	0.000	100.000	0.000	0.000	100
592	0.000	100.000	0.000	0.000	100
596	0.000	99.990	0.000	0.010	100
600	0.000	100.000	0.000	0.000	100
604	0.000	100.000	0.000	0.000	100
608	0.000	99.998	0.000	0.002	100
612	0.000	100.000	0.000	0.000	100
616	0.000	100.000	0.000	0.000	100
620	0.000	100.000	0.000	0.000	100
624	0.000	100.000	0.000	0.000	100
628	0.000	99.992	0.008	0.000	100
632	0.000	100.000	0.000	0.000	100
636	0.000	100.000	0.000	0.000	100
640	0.000	100.000	0.000	0.000	100
644	0.000	100.000	0.000	0.000	100
648	0.000	100.000	0.000	0.000	100
652	0.000	100.000	0.000	0.000	100
656	0.000	100.000	0.000	0.000	100
660	0.000	100.000	0.000	0.000	100
664	0.000	100.000	0.000	0.000	100
668	0.000	100.000	0.000	0.000	100
672	0.000	100.000	0.000	0.000	100
676	0.000	100.000	0.000	0.000	100
680	0.000	100.000	0.000	0.000	100
684	0.000	100.000	0.000	0.000	100
688	0.000	100.000	0.000	0.000	100
692	0.000	99.993	0.000	0.007	100
696	0.000	100.000	0.000	0.000	100
700	0.000	100.000	0.000	0.000	100
704	0.000	99.990	0.000	0.010	100
708	0.000	100.000	0.000	0.000	100
712	0.000	100.000	0.000	0.000	100
716	0.000	100.000	0.000	0.000	100
720	0.000	100.000	0.000	0.000	100

Position	Element				
(μm)	Cr	Ni	Al	Fe	Total
724	0.000	100.000	0.000	0.000	100
728	0.000	99.991	0.009	0.000	100
732	0.000	99.977	0.000	0.023	100
736	0.000	100.000	0.000	0.000	100
740	0.000	99.975	0.000	0.025	100
744	0.000	100.000	0.000	0.000	100
748	0.000	100.000	0.000	0.000	100
752	0.000	100.000	0.000	0.000	100
756	0.000	99.976	0.024	0.000	100
760	0.000	100.000	0.000	0.000	100
764	0.000	100.000	0.000	0.000	100
768	0.000	100.000	0.000	0.000	100
772	0.000	100.000	0.000	0.000	100
776	0.000	99.997	0.000	0.003	100
780	0.000	100.000	0.000	0.000	100
784	0.000	100.000	0.000	0.000	100
788	0.000	100.000	0.000	0.000	100
792	0.000	100.000	0.000	0.000	100
796	0.000	99.991	0.000	0.009	100
800	0.000	99.997	0.000	0.003	100

The location of the elemental line scan across a gap at the interface and the position of the interface between Alloy 214 and the nickel cladding are shown in Fig. A.1. The associated chemical information, obtained via wavelength-dispersive spectroscopy, is presented in Fig. A.2. The normalized atom percentage data are presented in Table A.2.

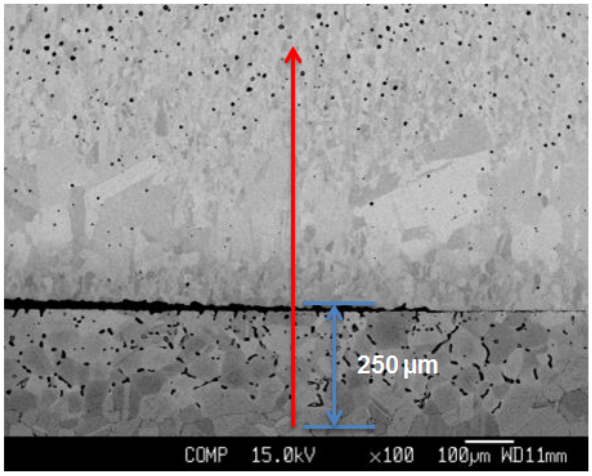

Fig. A.1. Image showing location of the elemental line scan across a gap in the interface (red arrow) and position of the interface between Alloy 214 and the nickel cladding with respect to the start of the line scan (blue arrow).

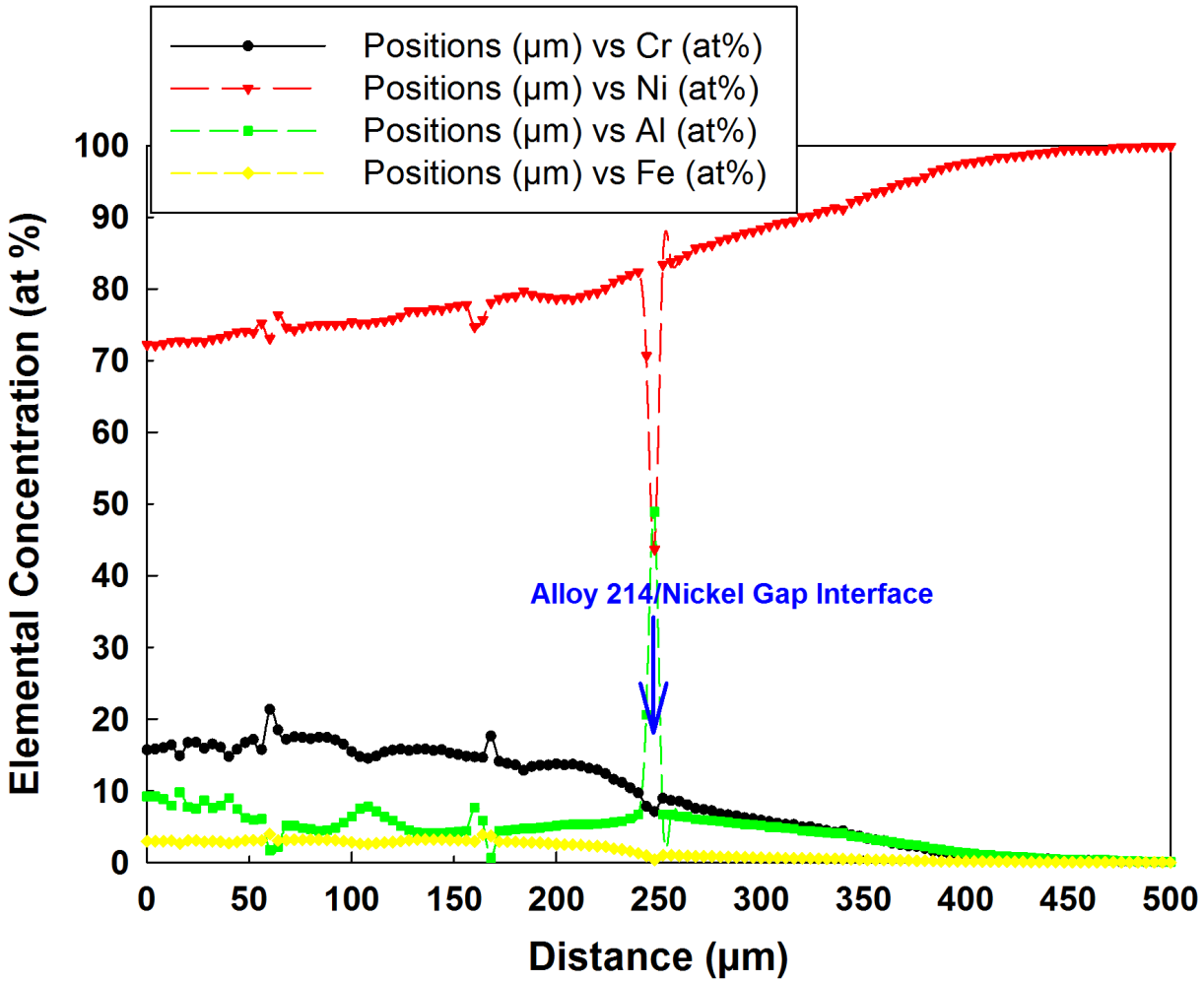

Fig. A.2. Normalized elemental concentration (at %) as a function of distance across gap interface. The interface between Alloy 214 and the nickel cladding (blue arrow) is at 250 μm.

Table A2. Elemental concentration (at. %) across gap interface of Alloy 214 and nickel cladding

Position	Element				
(um)	Cr	Ni	Al	Fe	Total
0	15.670	72.215	9.177	2.939	100
4	15.774	72.125	9.173	2.928	100
8	15.970	72.299	8.801	2.929	100
12	16.386	72.668	7.921	3.025	100
16	14.864	72.727	9.781	2.628	100
20	16.695	72.559	7.713	3.034	100
24	16.741	72.765	7.458	3.036	100
28	15.888	72.622	8.640	2.850	100
32	16.490	73.000	7.580	2.930	100
36	16.044	73.164	7.918	2.874	100

Position	Element				
(um)	Cr	Ni	Al	Fe	Total
40	14.755	73.584	8.976	2.684	100
44	15.758	73.992	7.407	2.843	100
48	16.690	74.091	6.175	3.044	100
52	17.132	73.898	5.891	3.079	100
56	15.735	75.203	6.029	3.033	100
60	21.320	73.064	1.671	3.946	100
64	18.465	76.344	2.136	3.055	100
68	17.161	74.647	5.086	3.105	100
72	17.498	74.243	5.094	3.165	100
76	17.415	74.657	4.795	3.132	100
80	17.236	74.953	4.646	3.165	100
84	17.446	74.987	4.396	3.171	100
88	17.404	75.015	4.458	3.122	100
92	17.063	75.025	4.821	3.091	100
96	16.480	75.008	5.545	2.967	100
100	15.437	75.362	6.422	2.779	100
104	14.717	75.192	7.512	2.579	100
108	14.512	75.179	7.761	2.547	100
112	14.804	75.423	7.103	2.670	100
116	15.375	75.523	6.356	2.745	100
120	15.645	75.715	5.836	2.804	100
124	15.799	76.188	5.066	2.947	100
128	15.589	76.862	4.487	3.061	100
132	15.760	76.912	4.160	3.167	100
136	15.797	76.964	4.058	3.181	100
140	15.583	77.220	4.043	3.154	100
144	15.701	77.105	4.032	3.162	100
148	15.257	77.464	4.172	3.106	100
152	15.051	77.652	4.237	3.059	100
156	14.781	77.795	4.395	3.029	100
160	14.714	74.710	7.636	2.940	100
164	14.605	75.687	5.855	3.853	100
168	17.618	78.043	0.627	3.712	100
172	14.085	78.650	4.388	2.877	100
176	13.787	78.877	4.452	2.884	100
180	13.572	78.975	4.575	2.879	100
184	12.816	79.672	4.718	2.794	100
188	13.363	79.167	4.725	2.745	100
192	13.521	78.921	4.826	2.733	100
196	13.571	78.812	4.970	2.647	100
200	13.729	78.626	5.096	2.549	100
204	13.587	78.701	5.235	2.476	100
208	13.659	78.554	5.303	2.484	100
212	13.406	78.880	5.302	2.412	100
216	13.093	79.295	5.303	2.308	100
220	12.904	79.508	5.327	2.260	100
224	12.346	80.048	5.431	2.175	100
228	11.567	80.958	5.577	1.899	100

Position	Element				
(um)	Cr	Ni	Al	Fe	Total
232	11.123	81.411	5.718	1.747	100
236	10.398	81.985	6.097	1.520	100
240	9.672	82.374	6.702	1.251	100
244	7.782	70.702	20.588	0.928	100
248	7.072	43.680	48.889	0.359	100
252	8.930	83.373	6.704	0.994	100
256	8.626	83.758	6.640	0.976	100
260	8.512	84.139	6.425	0.924	100
264	8.005	84.751	6.341	0.904	100
268	7.503	85.630	6.013	0.855	100
272	7.353	85.889	5.921	0.837	100
276	7.195	86.164	5.818	0.823	100
280	6.762	86.758	5.714	0.766	100
284	6.627	87.033	5.597	0.743	100
288	6.471	87.352	5.450	0.727	100
292	6.202	87.797	5.297	0.704	100
296	6.076	87.997	5.265	0.662	100
300	5.881	88.349	5.126	0.644	100
304	5.680	88.766	4.930	0.624	100
308	5.434	89.065	4.889	0.612	100
312	5.309	89.313	4.797	0.581	100
316	5.276	89.447	4.711	0.566	100
320	4.924	90.094	4.427	0.555	100
324	4.958	90.126	4.358	0.558	100
328	4.673	90.584	4.236	0.507	100
332	4.447	90.926	4.145	0.482	100
336	4.197	91.279	4.036	0.489	100
340	4.382	91.088	4.081	0.449	100
344	3.826	92.080	3.672	0.421	100
348	3.654	92.445	3.525	0.376	100
352	3.319	92.969	3.342	0.370	100
356	3.103	93.457	3.109	0.330	100
360	2.973	93.677	3.005	0.344	100
364	2.673	94.226	2.805	0.297	100
368	2.468	94.658	2.612	0.262	100
372	2.259	94.989	2.487	0.265	100
376	2.212	95.140	2.423	0.226	100
380	1.940	95.607	2.219	0.234	100
384	1.567	96.319	1.934	0.180	100
388	1.344	96.736	1.770	0.150	100
392	1.155	97.089	1.613	0.144	100
396	1.123	97.332	1.407	0.139	100
400	0.977	97.590	1.305	0.128	100
404	0.929	97.683	1.270	0.119	100
408	0.910	97.900	1.079	0.110	100
412	0.823	98.053	1.028	0.096	100
416	0.652	98.386	0.870	0.092	100
420	0.692	98.398	0.821	0.089	100

Position	Element				
(um)	Cr	Ni	Al	Fe	Total
424	0.618	98.518	0.791	0.073	100
428	0.584	98.599	0.749	0.068	100
432	0.515	98.807	0.625	0.053	100
436	0.437	98.927	0.597	0.039	100
440	0.444	99.018	0.503	0.034	100
444	0.295	99.219	0.457	0.030	100
448	0.224	99.381	0.368	0.028	100
452	0.194	99.410	0.371	0.025	100
456	0.218	99.418	0.339	0.026	100
460	0.242	99.426	0.305	0.028	100
464	0.244	99.402	0.336	0.019	100
468	0.237	99.407	0.343	0.013	100
472	0.073	99.674	0.240	0.014	100
476	0.028	99.746	0.215	0.011	100
480	0.047	99.775	0.178	0.000	100
484	0.026	99.814	0.147	0.013	100
488	0.004	99.860	0.136	0.000	100
492	0.009	99.848	0.139	0.005	100
496	0.026	99.855	0.111	0.009	100
500	0.028	99.904	0.069	0.000	100
504	0.038	99.891	0.071	0.000	100
508	0.051	99.827	0.101	0.021	100
512	0.000	99.924	0.067	0.009	100
516	0.000	99.953	0.044	0.003	100
520	0.004	99.907	0.089	0.000	100
524	0.000	99.981	0.016	0.003	100
528	0.000	99.988	0.013	0.000	100
532	0.000	99.954	0.047	0.000	100
536	0.000	99.973	0.016	0.011	100
540	0.000	99.979	0.021	0.001	100
544	0.000	100.000	0.000	0.000	100
548	0.000	100.000	0.000	0.000	100
552	0.000	100.000	0.000	0.000	100
556	0.000	100.000	0.000	0.000	100
560	0.000	99.991	0.009	0.001	100
564	0.000	99.998	0.000	0.002	100
568	0.000	99.993	0.000	0.007	100
572	0.000	99.993	0.007	0.000	100
576	0.000	99.866	0.134	0.000	100
580	0.000	99.997	0.000	0.003	100
584	0.000	99.995	0.005	0.000	100
588	0.000	100.000	0.000	0.000	100
592	0.000	100.000	0.000	0.000	100
596	0.000	100.000	0.000	0.000	100
600	0.000	99.994	0.000	0.006	100
604	0.000	99.987	0.013	0.000	100
608	0.000	100.000	0.000	0.000	100
612	0.000	99.978	0.012	0.010	100

Position	Element				
(um)	Cr	Ni	Al	Fe	Total
616	0.000	99.998	0.000	0.002	100
620	0.000	99.999	0.000	0.001	100
624	0.000	100.000	0.000	0.000	100
628	0.000	100.000	0.000	0.000	100
632	0.000	100.000	0.000	0.000	100
636	0.000	100.000	0.000	0.000	100
640	0.000	100.000	0.000	0.000	100
644	0.000	100.000	0.000	0.000	100
648	0.000	100.000	0.000	0.000	100
652	0.000	100.000	0.000	0.000	100
656	0.000	99.998	0.000	0.002	100
660	0.000	99.999	0.002	0.000	100
664	0.000	99.999	0.000	0.001	100
668	0.000	100.000	0.000	0.000	100
672	0.000	100.000	0.000	0.000	100
676	0.000	100.000	0.000	0.000	100
680	0.000	99.997	0.000	0.003	100
684	0.000	100.000	0.000	0.000	100
688	0.000	100.000	0.000	0.000	100
692	0.000	100.000	0.000	0.000	100
696	0.000	99.980	0.000	0.020	100
700	0.000	100.000	0.000	0.000	100
704	0.000	99.993	0.007	0.000	100
708	0.000	100.000	0.000	0.000	100
712	0.000	100.000	0.000	0.000	100
716	0.000	100.000	0.000	0.000	100
720	0.000	100.000	0.000	0.000	100
724	0.000	100.000	0.000	0.000	100
728	0.000	100.000	0.000	0.000	100
732	0.000	100.000	0.000	0.000	100
736	0.000	100.000	0.000	0.000	100
740	0.000	100.000	0.000	0.000	100
744	0.000	100.000	0.000	0.000	100
748	0.000	100.000	0.000	0.000	100
752	0.000	100.000	0.000	0.000	100
756	0.000	100.000	0.000	0.000	100
760	0.000	99.998	0.000	0.002	100
764	0.000	100.000	0.000	0.000	100
768	0.000	99.992	0.000	0.008	100
772	0.000	99.993	0.000	0.007	100
776	0.000	100.000	0.000	0.000	100
780	0.000	100.000	0.000	0.000	100
784	0.000	100.000	0.000	0.000	100
788	0.000	100.000	0.000	0.000	100
792	0.000	99.999	0.000	0.001	100
796	0.000	100.000	0.000	0.000	100
800	0.000	99.996	0.000	0.004	100